Energy & Environmental Science

PAPER

View Article Online
View Journal

Cite this: DOI: 10.1039/c4ee03907f

Scalable fabrication of efficient organolead trihalide perovskite solar cells with doctor-bladed active layers

Yehao Deng,† Edwin Peng,† Yuchuan Shao, Zhengguo Xiao, Qingfeng Dong* and Jinsong Huang*

Received 12th December 2014,
Accepted 18th March 2015

DOI: 10.1039/c4ee03907f

www.rsc.org/ees

Organolead trihalide perovskites (OTPs) are nature abundant materials with prospects as future low-cost renewable energy sources boosted by the solution process capability of these materials. Here we report the fabrication of efficient OTP devices by a simple, high throughput and low-cost doctor-blade coating process which can be compatible with the roll-to-roll fabrication process for the large scale production of perovskite solar cell panels. The formulation of appropriate precursor inks by removing impurities is shown to be critical in the formation of continuous, pin-hole free and phase-pure perovskite films on large area substrates, which is assisted by a high deposition temperature to guide the nucleation and grain growth process. The domain size reached 80–250 μm in 1.5–2 μm thick bladed films. By controlling the stoichiometry and thickness of the OTP films, highest device efficiencies of 12.8% and 15.1% are achieved in the devices fabricated on poly(3,4-ethylenedioxythiophene) polystyrene sulfonate and cross-linked *N*4,*N*4′-bis(4-(6-((3-ethyloxetan-3-yl)methoxy)hexyl)phenyl)–*N*4,*N*4′-diphenylbiphenyl-4,4′-diamine covered ITO substrates. Interestingly, the carrier diffusion length in doctor-bladed OTP films is beyond 3.5 μm which is significantly larger than in the spin-coated films, due to the formation of crystalline grains with a very large size by the doctor-blade coating method.

Broader context

Doctor-blade coating is a scalable, simple, low-cost, low temperature, solution based thin film deposition technique that is compatible with roll-to-roll fabrication of large area devices with a high throughput. Here we show that the large area (1 in × 1 in) organolead trihalide perovskite (OTP) solar cells can be fabricated by doctor-blade coating with a simple lab setup. We show that doctor-blade coating of OTP solar cells has advantages of much higher material usage efficiency, less contamination, unprecedented compatibility with different substrates, and easy control of the substrate temperature, which resulted in the formation of much larger crystalline grains than that obtained by the regular spin-coating method. The precursor formula and device interface engineering are also presented to boost the power conversion efficiency of the doctor-bladed OTP solar cell to above 15%. This method for OTP solar cell fabrication opens up a new room to design experiments with better control of parameters such as OTP film thickness, stoichiometric ratio, solvent evaporation rate, *etc.*, paving the road for the scaling up of the fabrication and commercialization of OTP solar cells.

Introduction

Thin film photovoltaic devices based on organometal trihalide perovskites (OTPs) are a very promising area of renewable energy research.[1–5] These solar cells utilize light harvesting thin films composed of polycrystalline perovskites with a structure of AMX_3, where A is an organic cation, usually methylammonium ($CH_3NH_3^+$, MA^+), M is the metal cation, commonly Pb^{2+}, and X is the halide anion (I^-, Cl^-, and/or Br^-).[1,6,7] The reported highest power conversion efficiencies (PCE) of perovskite solar cells quickly increased to above 16%.[4,8,9] The solution processability of OTPs enables the capitalization of development in organic photovoltaics (OPVs) for future low-cost, high-throughput production of OTP solar panels on both rigid and flexible substrates. However, current methods for fabricating high efficiency perovskite solar cells, such as spin-coating or thermal evaporation, are not compatible with large-scale production processes such as the roll-to-roll process.[10–13] Some cost-effective and scalable fabrication methods for perovskite solar cells, including ultrasonic

Department of Mechanical and Materials Engineering, University of Nebraska-Lincoln, Lincoln, Nebraska 68588-0656, USA. E-mail: jhuang2@unl.edu, qingfeng.dong@gmail.com

† These authors contributed to this work equally.

spray-coating and inkjet-printing, were reported recently to successfully fabricate perovskite cells, but the PCEs of the fabricated devices were much lower than that of those fabricated by spin-coating.[10,14,15]

Here we report the fabrication of high efficiency perovskite solar cells using a doctor blade method. Doctor-blade deposition has been used prevalently for various thin films in other types of thin film solar cells.[16–20] The appeal for utilizing doctor blading is primarily due to scalability for roll-to-roll production, simplicity, and cost effectiveness.[17,18] Furthermore, doctor-blading also has the advantages of high throughput deposition, high material usage, and application onto flexible substrates.[16,18,19] Here we investigated doctor-blading with the goal of achieving such benefits for OTP deposition. Solar cells made using bladed $MAPbI_3$ films achieved a maximum PCE of 15.1%. Furthermore, we demonstrated that this technique can be easily adapted for a wide variety of perovskite chemistries, substrates, and device structures.

Results and discussion

Fig. 1a shows the setup for doctor blade coating perovskite films onto indium tin oxide (ITO) glass substrates. The precursor solution was PbI_2 and methylammonium iodide (CH_3NH_3I, MAI) dissolved in dimethylformamide (DMF). In the coating process, a precursor solution was dropped onto hole transport material covered ITO substrates, and swiped linearly by a glass blade at a high speed of 0.75 cm s^{-1} (27 m h^{-1}). Such a high deposition speed is attractive in fabricating large area perovskite solar panels with a high throughput. The substrates were held at elevated temperature during doctor-blade deposition for the

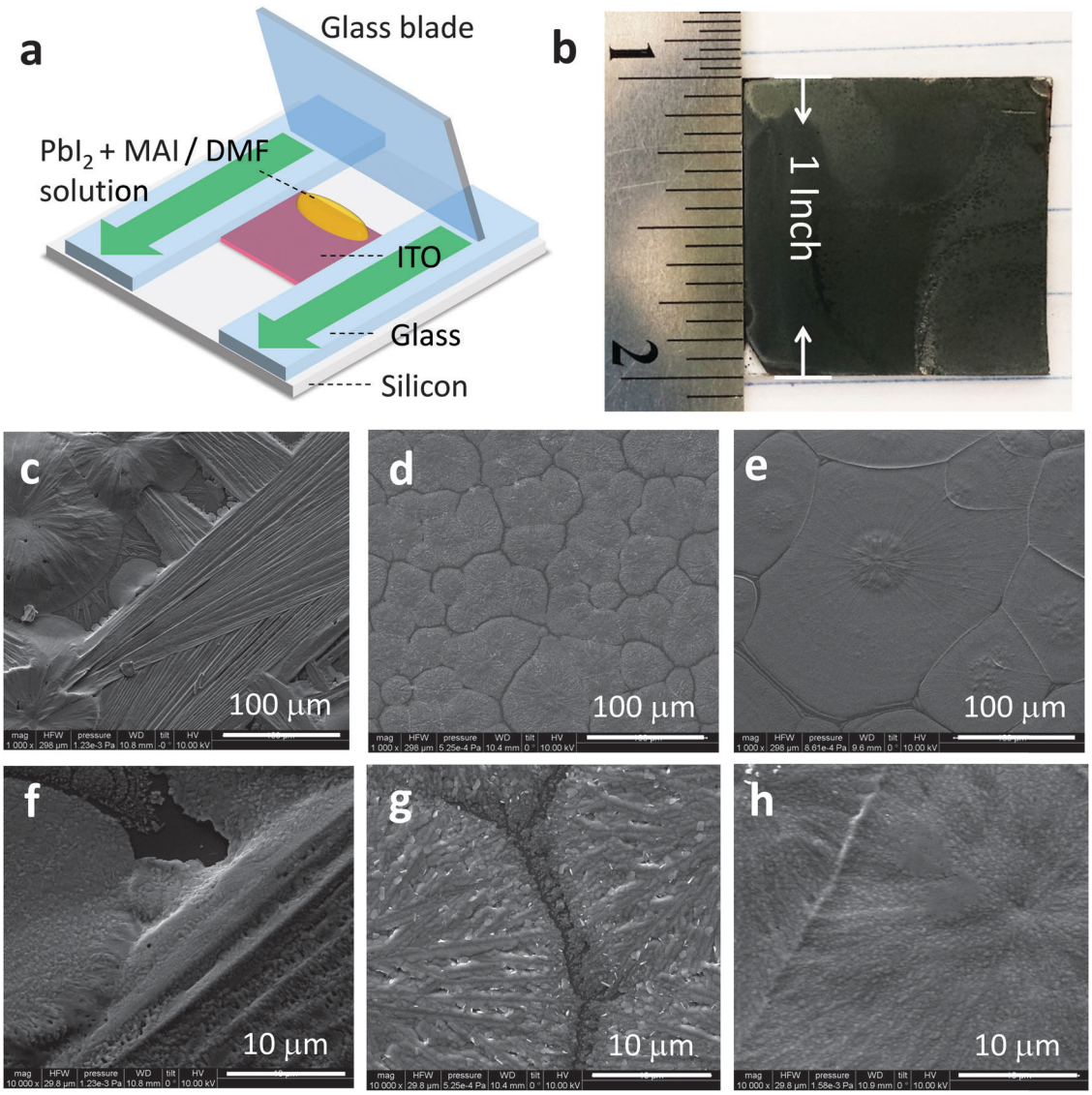

Fig. 1 (a) Illustration of the experimental setup for perovskite film deposition *via* doctor-blading. (b) A picture of the large area (1 inch × 1 inch) film formed by doctor-blade coating; (c, f) SEM images of $MAPbI_3$ films formed at a low temperature of 100 °C; (d, g) SEM images of $MAPbI_3$ films formed at a low temperature of 125 °C using unpurified MAI; (e, h) SEM images of $MAPbI_3$ films formed at a low temperature of 125 °C using purified MAI.

formation of smooth, pin-hole free OTP films. The thickness of the OTP films during doctor-blade coating was controlled by perovskite precursor solution concentration, blading speed and the spacing of the doctor-blade and the substrates. Typically, 10–20 μL of precursor solution was used for a 2.25 cm^2 substrate. This was much lower than 50–100 μL typically used for the spin-coating of the same perovskite solution over the same area substrate, which demonstrated the advantages of the much higher material usage rate by doctor-blade coating. For doctor-blade deposition, the substrate temperature was another important parameter for creating uniform, smooth and pin-hole free OTP films. When the ITO substrate was held at a temperature much lower than the boiling point of DMF (153 °C), the OTP film drying time was too long, and the quick crystallization of OTPs created very rough, discontinuous films. As shown by the scanning electron microscopy (SEM) images in Fig. 1c and f, the OTP films formed at 100 °C are non-uniform, and contain numerous ~μm wide pinholes, which yielded very low device PCE below 7%. A quick drying of the OTP films within 2 seconds can create uniform and continuous films. OTP films deposited at 125 °C, which was the optimum temperature for doctor-blade coating, are clearly continuous and smooth (Fig. 1d, e, g and h). Very high temperature is avoided because it might cause the rapid decomposition of $CH_3NH_3PbI_3$ ($MAPbI_3$).

Purification of MAI is not necessary for spin-coating fabrication of high efficiency $MAPbI_3$ devices using our previously demonstrated two-step interdiffusion method[21] or single step method,[22] but it is found to be crucial for the doctor-blade coating of the smooth OTP films. Precursor solutions made from PbI_2 and non-purified MAI become immediately visibly cloudy, even after filtration of the precursor solution with a 0.2 μm pore size filter. This is most likely caused by the reaction of Pb^{2+} with impurity $H_2PO_2^-$ that forms insoluble $Pb(H_2PO_3)_2$ particles. Generally, HI and CH_3NH_2 (MA) solutions are used as the starting materials for MAI synthesis, while the HI solution contains ~1.5% H_3PO_2 (Sigma-Aldrich) as a stabilizer to prevent the decomposition of HI. H_3PO_2 or its reaction product with MA, MAH_2PO_3, is hard to be completely removed by the regular MAI washing process using diethyl ether. In order to remove the impurities, here we purified MAI by recrystallization, *i.e.*, cooling the high-temperature supersaturated MAI solution in ethanol to obtain large purified MAI crystals. Due to the very high solubility of H_3PO_2 and MAH_2PO_2 in ethanol, H_3PO_2 and MAH_2PO_2 cannot be recrystallized and thus remain in the ethanol solution. Precursor solutions made from PbI_2 with purified MAI in DMF appear very clear without visible appearance change after storage for several months under ambient conditions. The SEM pictures of the doctor-blade coated films from both types of solution are shown in Fig. 1d, e, g and h. The produced films from non-purified MAI were non-continuous with micrometer wide gaps in between the large domains which might be impurities pushed toward the edges during the grain growth process. In sharp contrast, the films deposited from purified MAI have no any gaps between big domains (Fig. 1e and h). Devices made with non-purified MAI performed significantly worse due to shunting paths from direct contact between the PEDOT:PSS film and the cathode.[23] It should be noted that these blade-coated films have a unique domain structure with very large hexagonal shape domains with lateral size in the order of 80–250 μm. Judging from the surface topography of the domains, we speculate that the grains nucleate and grow from the centers with a spacing of 80–250 μm, and quickly merged with each other to form large domains. The absence of impurity resulted in good connection of these domains without any gaps (Fig. 1h). Each hexagonal domain still contains multiple grains which will be illustrated by the cross-section SEM pictures. By controlling the substrate temperature, blading speed, precursor solution concentration, and using purified MAI mixed with PbI_2 solution, we were able to coat 1 inch × 1 inch OTP films on rigid ITO substrates with film thickness in the range of 0.2 μm to over 10 μm, as shown by the picture in Fig. 1b.

After achieving good film morphology with right deposition temperature and purified precursor, we fabricated OTP solar cell devices to evaluate the films made from the doctor-blade deposited OTP films. A device structure ITO/poly(3,4-ethylenedioxythiophene) polystyrene sulfonate (PEDOT:PSS)/$MAPbI_3$/[6,6]-phenyl-C61-butyric acid methyl ester ($PC_{60}BM$ 10 nm)/C_{60} (20 nm)/2,9-dimethyl-4,7-diphenyl-1,10-phenanthroline (BCP, 8 nm)/aluminum (Al, 100 nm) was used which is shown in Fig. 2a.[21,24,25] It was previously found that a non-stoichiometric precursor solution is critical for the formation of $MAPbI_3$ films by a single-step spin-coating process from a mixed precursor solution, and a PbI_2 : MAI molar ratio of 0.6–0.7 resulted in most efficient devices.[21] This is due to the different affinity of MAI and PbI_2 to the PEDOT:PSS substrate, a greater amount of MAI than PbI_2 in the precursor solution is needed to form stoichiometric $MAPbI_3$ films.[22] In order to find out whether this is still valid

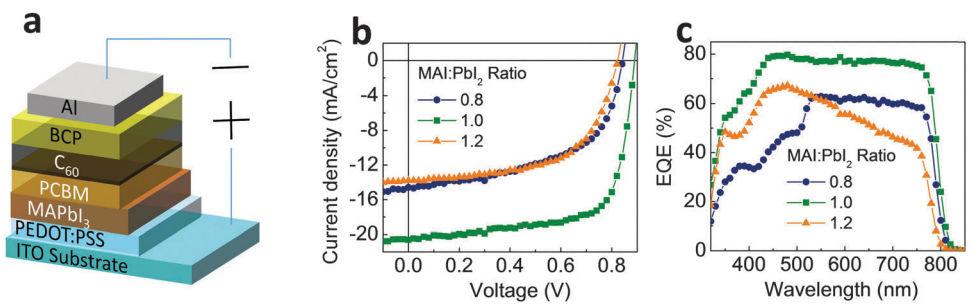

Fig. 2 (a) Device structure; (b) Photocurrent curves of the doctor-blade coated devices under 1 sun condition and (c) EQE spectrum of top devices made from 1.0 : 08, 1.0 : 1.0, and 1.0 : 1.2 PbI_2 : MAI molar ratio solution.

in doctor-blade coating, we varied the ratio of MAI to PbI_2 in the precursor solution, and studied its influence on OTP device performance. Here all other experimental parameters were kept unchanged and only the MAI : PbI_2 molar ratio was changed. The photocurrent and external quantum efficiency spectra of the devices with different MAI : PbI_2 molar ratios of 0.8, 1.0 and 1.2 are shown in Fig. 2b and c. It shows clearly that the stoichiometry of the precursor solution resulted in the highest device performance. This difference can be explained by the fact that all PbI_2 and MAI are forced to stay in the doctor-blade deposited $MAPbI_3$ films, while it is very likely that more MAI could be spun off the substrates in the spin-coating process or be evaporated during the thermal annealing process.

Finally, we studied the influence of film thickness on the device performance by tuning the thickness of the OTP layer with varied spacing between the substrate and the blading glass slides, yielding a wide thickness range from 175 nm to 9.6 μm. Fig. 3a and b show the photocurrent and external quantum efficiency (EQE) curves of the devices with OTP thicknesses of 0.6, 1.0, 2.0, 3.0, 3.7 and 5.6 μm obtained from 1 : 1 (molar ratio) PbI_2 : MAI precursor solution, and Fig. 3c and f depict device performance statistics, including PCE, fill factor (FF), short circuit current (J_{SC}), and open circuit voltage (V_{OC}), *versus* $MAPbI_3$ film thickness. All of these parameters first increased and then decreased with increasing $MAPbI_3$ film thickness, although they reached a maximum at different $MAPbI_3$ film thicknesses. Such variation trend can be explained by the definite tradeoff between the stronger light absorption induced larger photocurrent and increased charge recombination which resulted in lower photocurrent and photovoltage as the film thickness increases. The trend of PCE as a function of $MAPbI_3$ thickness was strongly correlated with the trend of J_{SC}. At $MAPbI_3$ thickness between 1.5 and 3.5 μm, J_{SC} was almost constant above 20 mA cm^{-2}. The best performing device was 3.1 μm thick with a PCE of 12.8%. Maximum V_{OC} (0.88 V) was observed at a slightly higher $MAPbI_3$ thickness in the range of 2 to 5 μm. A similar trend between PCE and thickness was observed for perovskite devices made using the spin-coating interdiffusion method or co-evaporation method,[22,25,26] while with doctor-blade deposition, the optimum $MAPbI_3$ thickness is much greater than that for same-structure devices made by the spin-coating method (630 nm).[25] This indicates that the doctor-bladed $MAPbI_3$ films have a much longer carrier diffusion length along the out of film plane direction than the spun film. 3.5 μm is the longest carrier diffusion length demonstrated for $MAPbI_3$ based polycrystalline solar cells. In order to verify the device efficiency, we measured the steady state photocurrent of one device at its maximum power point (0.68 V) (Fig. 3g). As shown in Fig. 3h, the photocurrent rose quickly when light is on, and the stabilized photocurrent is the same as that read from the photocurrent scanning (Fig. 3g).

In order to understand the origin of the much longer carrier diffusion length in $MAPbI_3$ films by doctor-blade coating than that obtained by spin-coating following the interdiffusion

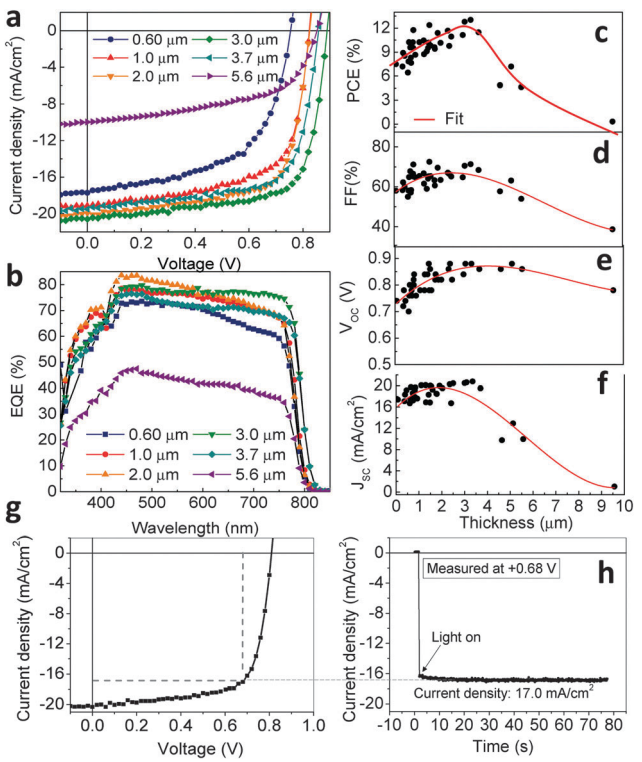

Fig. 3 (a) Photocurrent curves under 1 sun condition and (b) EQE spectra of devices made from 0.6 to 5.6 μm thick perovskite films. Dependence of (c) PCE, (d) FF, (e) V_{OC}, and (f) J_{SC} on perovskite films of thickness from 0.2 to 9.5 μm in devices with fitting curves for eye guidance. (g, h) Verification of the power conversion efficiency by measuring the steady-state (stabilized) photocurrent density at maximum power point.

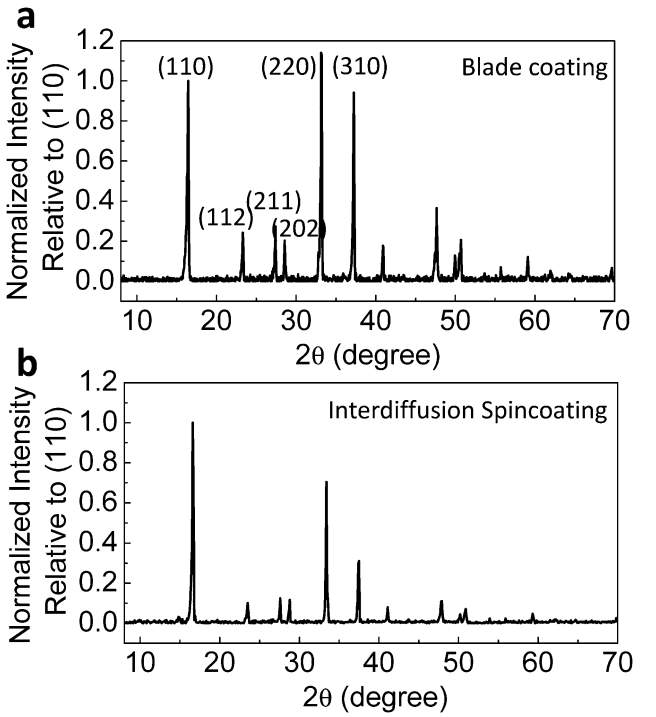

Fig. 4 Normalized XRD spectra of the $MAPbI_3$ films formed by doctor blade coating (a) and interdiffusion spin-coating (b) methods with intensity normalized by that of the (110) peak.

process, we examined the differences of the structure and morphology properties of the films formed by these two methods. Fig. 4 shows X-ray diffraction (XRD) spectra of solvent-annealed $MAPbI_3$ films deposited with doctor-blade and interdiffusion spin-coating. The intensities were normalized to the magnitude of the peak from the (110) plane. The same XRD patterns indicate that the doctor-blade perovskite films are of the tetragonal *I*4/*mcm* structure, same as that of the spun film.[6,25] There was however higher intensity of other planes, particularly the (220) plane, relative to the (110) peak for doctor-blade films, indicating that the grain orientation distribution is different in both types of films. The preferred (220) grain growth was also observed in mixed halide perovskite films induced by the incorporation of Cl, where more (220) grains were found to enhance the carrier recombination lifetime.[27] Here these grain orientation differences can be explained by the disparate methodologies. Interdiffusion spin-coating is a two-step process (first PbI_2, then MAI) and occurs at elevated temperature over a very long annealing time of over 45 min where the grain orientation of PbI_2 might influence that of formed $MAPbI_3$ grains. Grain formation in doctor blade deposition is done with one step in a very short period of less than 2 seconds, and surface tension force from the blade might cause the alignment of crystals during the blade-coating process which were observed previously in very thin organic films formed by a similar process.[28,29]

A SEM image of a 2.5 μm thick doctor blade coated film is shown in Fig. 5a with grain size distribution from 250 nm to 2250 nm along with that from a 1 μm thick perovskite film made by interdiffusion spincoating is shown in Fig. 5b. The doctor-blade coated films have a much larger distribution of grain size than the films formed by the interdiffusion method. The largest grain size reached above 3 μm. The cross-section SEM images of the doctor-bladed coated films are also shown in Fig. 5c. Similar to the films formed by solvent-annealed interdiffusion,[25] most grains connect the anode and cathode directly without grain-boundaries in the out-of-plane direction, which facilitates the photogenerated charge extraction and explains the ultra-long charge diffusion length observed. The doctor-blade coating produces films with a wider range of grain size distribution as well as much larger grain with the largest grain lateral size comparable to the film thickness (2–3 μm). Most of the areas of the doctor-blade coated films are covered by the large size grains, which can effectively reduce the charge recombination at grain boundaries and reduce charge recombination, contributing to the much longer charge diffusion length observed. However the presence of many small grains might still limit the overall device efficiency because it is easy for photogenerated charges to diffuse into these grain boundaries which are the sink of charges.

To demonstrate the scalability of our doctor-blade coating method, we fabricated OTPs devices on large area (1 inch × 1 inch) doctor-blade coated films. The thickness of the OTP layer was maintained at 2–3 μm. As shown in Fig. 6a, the active area of the devices is depicted by red dotted rectangles. The normalized PCE distribution is shown in Fig. 6b. We can see that the PCE is generally consistent over the areas investigated, the difference between the highest and lowest PCE is within 25%, showing that this method can be compatible with the roll-to-roll fabrication process for the large scale production of perovskite solar cell panels. The minor decrease in PCE from the edge to the center may be explained by the increased resistance of ITO which causes voltage reduction due to the series resistance.

The PCE of the OTP devices made on the PEDOT:PSS hole transport layer (HTL) is limited by the low V_{OC}. We further improved the solar cell device performance with better HTLs. From our previous study of the influence of HTL on OTP device performance with the interdiffusion spin-coat method, it was found that using cross-linked *N*4,*N*4′-bis(4-(6-((3-ethyloxetan-3-yl)methoxy)hexyl)phenyl)–*N*4,*N*4′-diphenylbiphenyl-4,4′-diamine (c-OTPD) in place of PEDOT:PSS significantly improved the V_{OC}, and therefore the PCE of OTP solar cells.[31] However, continuous OTP films were proved to be much more difficult to form on c-OTPD with doctor-blade deposition as the OTP solution cannot wet the hydrophobic c-OTPD surface, resulting in a much lower yield of pin-hole free, continuous OTP films on c-OTPD *versus* on PEDOT:PSS. To address this issue, we incorporated 0.20 wt% (*z*)-2-cyano-3-(4-(diphenylamino)phenyl)acrylic acid (TPACA) into the c-OTPD solution. The chemical structure of TPACA is shown in Fig. 7a. Due to the strong polarity and carboxyl group in

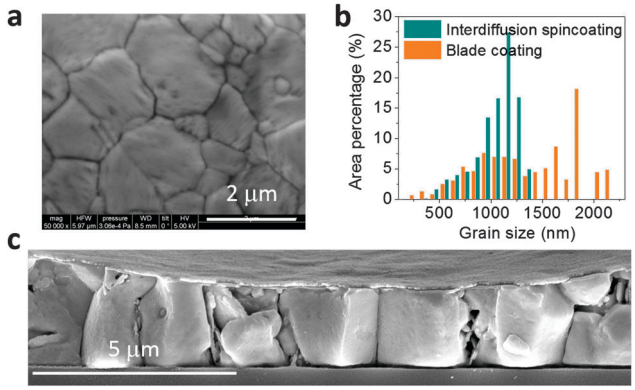

Fig. 5 (a) Top surface SEM of a doctor blade coated film with a thickness of 2.5 μm. (b) Perovskite grain size statistics of doctor blade and interdiffusion spin-coated films. Here the area percentages of these grains are shown; (c) cross-section SEM images of devices made from doctor-blade coating.

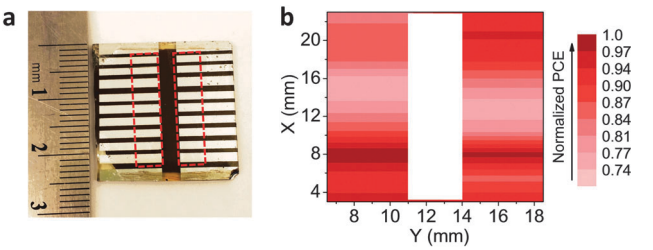

Fig. 6 (a) A picture of large area (1 inch × 1 inch) doctor-blade coated OTP device. The red dotted rectangles indicate the active areas. (b) PCE distribution contour on the active areas.

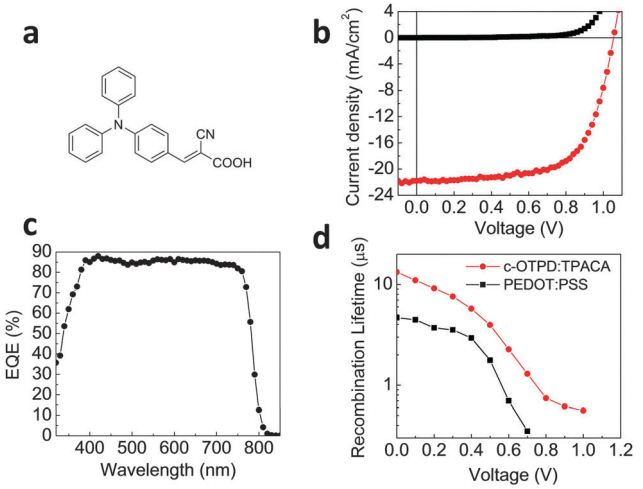

Fig. 7 (a) Molecular structure of TPACA. (b) Photocurrent curves of the device under 1 sun illumination and dark conditions, and (c) EQE spectrum of the ITO/c-OTPD:TPACA/$MAPbI_3$/$PC_{60}BM$/C_{60}/BCP/Al. (d) Charge recombination lifetime comparison of doctor blade devices with c-OTPD:TPACA and PEDOT:PSS HTLs.

TPACA, the resulting c-OTPD:TPACA HTL is much more hydrophilic, which significantly improved the OTP film yield when using doctor blade deposition. Using the c-OTPD:TPACA HTL resulted in the best device performance. As shown in Fig. 7b, the champion cell with a $MAPbI_3$ thickness of 845 nm has a PCE of 15.1%. Both V_{OC} of 1.05 V and J_{SC} of 21.8 mA cm^{-2} were substantially higher than what was achieved with PEDOT:PSS HTL. The EQE of the device is above 85% in a wide range of wavelength and the EQE curve is almost flat in the absorption band (Fig. 7c). Our improved device using c-OTPD based HTL demonstrates that our doctor-blade technique is applicable for deposition over different interfacial layers and can be adapted for other perovskite solar cell structures. We attribute the increased efficiency in the device using c-OTPD:TPACA HTL to the much weaker charge recombination and high work function of c-OTPD. Fig. 7d depicts the charge recombination lifetime, as measured by impedance spectroscopy, *versus* bias voltage for the champion c-OTPD:TPACA device and for the PEDOT:PSS device with the same perovskite thickness.[30] The charge recombination lifetime is in the same range with those made by spin-coating.[25] Clearly the charge recombination lifetime is much longer in the device with c-OTPD HTL. A similar increase in charge recombination lifetime was also observed in the interdiffusion formed planar heterojunction devices with c-OTPD HTL,[31] which indicates a general function of the c-OTPD layer that can improve the crystal quality of OTP films and reduce charge traps.

In summary, we demonstrated that continuous, large grain size $MAPbI_3$ films could be fabricated by the doctor-blade technique and the maximum PCE of the solar cells with such films reached 15.1%. The perovskite films were deposited faster, using lower energy, and requiring smaller amounts of precursor solution compared to the interdiffusion spincoating method. $MAPbI_3$ films made with doctor-blade coating on PEDOT:PSS have extremely long carrier diffusion length up to 3.5 μm. Such doctor-blade deposition can be applied for large area perovskite cells fabricated with high volume roll-to-roll production.

Experimental section

The perovskite photovoltaic devices had a structure of ITO/HTL/$MAPbI_3$/[6,6]-phenyl-C61-butyric acid methyl ester ($PC_{60}BM$)/C_{60}/2,9-dimethyl-4,7-diphenyl-1,10-phenanthroline (BCP)/Al. Indium tin oxide (ITO) coated glass substrates were cleaned successively with deionized water, acetone, and UVO cleaner (Jelight 42). HTL was either PEDOT:PSS or c-OTPD plus TPACA. PEDOT:PSS was spincoated onto ITO substrates at 3000 rpm for 50 s and dried in air at 135 °C for 20 min. We deposited a 15 nm thick c-OTPD layer with 0.25 wt% TPACA 1,2-dichlorobenzene (DCB) solution onto an ITO substrate using spin-coating. Then, the c-OTPD film was cross-linked using a UV lamp and dried in N_2 at 100 °C for 10 min.

Perovskite and fullerene layers were deposited on top of the PEDOT:PSS or c-OTPD:TPACA layer inside a N_2 atmosphere. In the doctor blade coating process, the precursor solution was dropped onto the HTL-covered ITO substrate, and swiped linearly by a glass blade at a high speed of 0.75 cm s^{-1} (27 m h^{-1}). The substrates were held at elevated temperature during blade deposition (typically 125 °C). The thickness of the perovskite films during blade coating was controlled by perovskite precursor solution concentration and the depth of the blading channel. Methylammonium iodide (CH_3NH_3I, MAI) and PbI_2 dissolved in dimethylformamide (DMF) were used as the perovskite precursor solution. We primarily use 1 : 1 molar ratio between PbI_2 and methylammonium halide, at a mass ratio of 40% PbI_2 (400 mg per 1 mL DMF) and 13.8% methylammonium halide. We used 10–20 μL of precursor solution per 2.25 mm^2 substrate. This was much lower than 50–100 μL typically used for spin coating of similar perovskite solutions over the same area substrate, which demonstrated the advantages of high material usage by doctor-blade coating.[22,25]

The as-deposited perovskite films were subsequently thermally annealed at 100 °C for 60 minutes while undergoing solvent annealing with 10 μL of DMF according to our previously reported method.[25] $PC_{60}BM$, dissolved in 2% by weight DCB solution, was spin-coated on top of the perovskite layer at 6000 rpm for 35 s. The resulting film was further thermally annealed at 100 °C for 60 minutes without solvent annealing. C_{60} (20 nm thick) and BCP (8 nm) were deposited by thermal evaporation. Finally, 100 nm Al was deposited with a mask to provide a cell area of 7.25 mm^2 for majority of our devices.

We used simulated AM 1.5G irradiation provided by a xenon lamp (Oriel 67005) to measure the photocurrent of our devices. The light intensity was calibrated using a Si diode (Hamamatsu S1133). The current–voltage (*IV*) relationship was measured using a source-meter (Keithley 2400), with our standard test procedure of scanning at 0.2 V s^{-1}. The external quantum efficiency (EQE) was obtained using a Newport QE measurement kit. Impedance spectroscopy measurements were made using a LCR meter (Agilent E4980A) under the simulated 1 sun irradiation.[31] A Rigaku D/Max-B Diffractometer with Co K_α was

used to perform X-ray diffraction (XRD). Topographical and cross-section SEM (Quanta 200 FEG ESEM) imaging was performed after sputtering of Au onto samples (Cressington 108). The film thickness was measured by stylus profilometry (Bruker Dektak XTL).

Acknowledgements

We thank the Department of Energy under Award DE-EE0006709, the National Science Foundation for the financial support provided under Awards ECCS-1252623 and ECCS-1201384, and the Nebraska Public Power District through the Nebraska Center for Energy Sciences Research.

References

1 V. Gonzalez-Pedro, E. J. Juarez-Perez, W.-S. Arsyad, E. M. Barea, F. Fabregat-Santiago, I. Mora-Sero and J. Bisquert, *Nano Lett.*, 2014, **14**, 888–893.
2 G. Hodes, *Science*, 2013, **342**, 317–318.
3 P. V. Kamat, *J. Am. Chem. Soc.*, 2014, **136**, 3713–3714.
4 M. D. McGehee, *Nat. Mater.*, 2014, **13**, 845–846.
5 Y. Shao, Z. Xiao, C. Bi, Y. Yuan and J. Huang, *Nat. Commun.*, 2014, **5**, 5784.
6 T. Baikie, Y. Fang, J. M. Kadro, M. Schreyer, F. Wei, S. G. Mhaisalkar, M. Graetzel and T. J. White, *J. Mater. Chem. A*, 2013, **1**, 5628–5641.
7 P. P. Boix, K. Nonomura, N. Mathews and S. G. Mhaisalkar, *Mater. Today*, 2014, **17**, 16–23.
8 M. A. Green, A. Ho-Baillie and H. J. Snaith, *Nat. Photonics*, 2014, **8**, 506–514.
9 H. Zhou, Q. Chen, G. Li, S. Luo, T.-b. Song, H.-S. Duan, Z. Hong, J. You, Y. Liu and Y. Yang, *Science*, 2014, **345**, 542–546.
10 M. R. Leyden, L. K. Ono, S. R. Raga, Y. Kato, S. Wang and Y. Qi, *J. Mater. Chem. A*, 2014, **2**, 18742–18745.
11 M. Liu, M. B. Johnston and H. J. Snaith, *Nature*, 2013, **501**, 395–398.
12 O. Malinkiewicz, C. Roldán-Carmona, A. Soriano, E. Bandiello, L. Camacho, M. K. Nazeeruddin and H. J. Bolink, *Adv. Energy Mater.*, 2014, **4**, DOI: 10.1002/aenm.201400345.
13 O. Malinkiewicz, A. Yella, Y. H. Lee, G. M. Espallargas, M. Graetzel, M. K. Nazeeruddin and H. J. Bolink, *Nat. Photonics*, 2014, **8**, 128–132.
14 A. T. Barrows, A. J. Pearson, C. K. Kwak, A. D. Dunbar, A. R. Buckley and D. G. Lidzey, *Energy Environ. Sci.*, 2014, **7**, 2944–2950.
15 A. Mei, X. Li, L. Liu, Z. Ku, T. Liu, Y. Rong, M. Xu, M. Hu, J. Chen and Y. Yang, *Science*, 2014, **345**, 295–298.
16 T. Brown, F. De Rossi, F. Di Giacomo, G. Mincuzzi, V. Zardetto, A. Reale and A. Di Carlo, *J. Mater. Chem. A*, 2014, **2**, 10788–10817.
17 I. Burgués-Ceballos, M. Stella, P. Lacharmoise and E. Martínez-Ferrero, *J. Mater. Chem. A*, 2014, **2**, 17711–17722.
18 M. Kaelin, D. Rudmann and A. Tiwari, *Sol. Energy*, 2004, **77**, 749–756.
19 A. Schneider, N. Traut and M. Hamburger, *Sol. Energy Mater. Sol. Cells*, 2014, **126**, 149–154.
20 K. Xiong, L. Hou, M. Wu, Y. Huo, W. Mo, Y. Yuan, S. Sun, W. Xu and E. Wang, *Sol. Energy Mater. Sol. Cells*, 2015, **132**, 252–259.
21 Z. Xiao, C. Bi, Y. Shao, Q. Dong, Q. Wang, Y. Yuan, C. Wang, Y. Gao and J. Huang, *Energy Environ. Sci.*, 2014, **7**, 2619–2623.
22 Q. Wang, Y. Shao, Q. Dong, Z. Xiao, Y. Yuan and J. Huang, *Energy Environ. Sci.*, 2014, **7**, 2359–2365.
23 J. M. Ball, M. M. Lee, A. Hey and H. J. Snaith, *Energy Environ. Sci.*, 2013, **6**, 1739–1743.
24 Z. Xiao, Y. Yuan, Y. Shao, Q. Wang, Q. Dong, C. Bi, P. Sharma, A. Gruverman and J. Huang, *Nat. Mater.*, 2015, **14**, 193–198.
25 Z. Xiao, Q. Dong, C. Bi, Y. Shao, Y. Yuan and J. Huang, *Adv. Mater.*, 2014, **26**, 6503–6509.
26 C. Momblona, O. Malinkiewicz, C. Roldán-Carmona, A. Soriano, L. Gil-Escrig, E. Bandiello, M. Scheepers, E. Edri and H. J. Bolink, *APL Mater.*, 2014, **2**, 081504.
27 Q. Dong, Y. Yuan, Y. Shao, Y. Fang, Q. Wang and J. Huang, *Energy Environ. Sci.*, 2015, under review.
28 Y. Diao, B. C. Tee, G. Giri, J. Xu, D. H. Kim, H. A. Becerril, R. M. Stoltenberg, T. H. Lee, G. Xue and S. C. Mannsfeld, *Nat. Mater.*, 2013, **12**, 665–671.
29 Y. Yuan, G. Giri, A. L. Ayzner, A. P. Zoombelt, S. C. Mannsfeld, J. Chen, D. Nordlund, M. F. Toney, J. Huang and Z. Bao, *Nat. Commun.*, 2014, **5**, 3005.
30 I. Mora-Seró, G. Garcia-Belmonte, P. P. Boix, M. A. Vázquez and J. Bisquert, *Energy Environ. Sci.*, 2009, **2**, 678–686.
31 C. Bi, Q. Wang, Y. Shao, Y. Yuan, Z. Xiao and J. Huang, under review.